Separation of Actinides from Rare Earth Elements by Electrorefining in LiC1KC1 Eutectic Salt

Article *in* Journal of Nuclear Science and Technology · January 1998

DOI: 10.1080/18811248.1998.9733819

10 authors, including:

Takatoshi Hijikata
Central Research Institute of Epidemiology
29 PUBLICATIONS **627** CITATIONS
SEE PROFILE


Tadashi Inoue
Central Research Institute of Electric Power Industry
50 PUBLICATIONS **1,830** CITATIONS
SEE PROFILE

Steve Fusselman
Aerospace Corporation
23 PUBLICATIONS **714** CITATIONS
SEE PROFILE

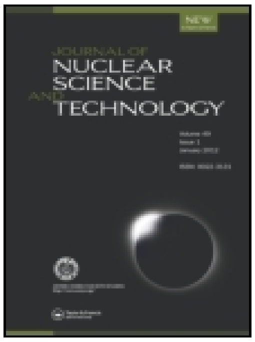

Taylor & Francis
Taylor & Francis Group

Journal of Nuclear Science and Technology

ISSN: 0022-3131 (Print) 1881-1248 (Online) Journal homepage: http://www.tandfonline.com/loi/tnst20

Separation of Actinides from Rare Earth Elements by Electrorefining in LiC1-KC1 Eutectic Salt

Yoshiharu SAKAMURA , Takatoshi HIJIKATA , Kensuke KINOSHITA , Tadashi INOUE , T. S. STORVICK , C. L. KRUEGER , L. F. GRANTHAM , S. P. FUSSELMAN , D. L. GRIMMETT & J. J. ROY

To cite this article: Yoshiharu SAKAMURA , Takatoshi HIJIKATA , Kensuke KINOSHITA , Tadashi INOUE , T. S. STORVICK , C. L. KRUEGER , L. F. GRANTHAM , S. P. FUSSELMAN , D. L. GRIMMETT & J. J. ROY (1998) Separation of Actinides from Rare Earth Elements by Electrorefining in LiC1-KC1 Eutectic Salt, Journal of Nuclear Science and Technology, 35:1, 49-59, DOI: 10.1080/18811248.1998.9733819

To link to this article: http://dx.doi.org/10.1080/18811248.1998.9733819

Journal of NUCLEAR SCIENCE and TECHNOLOGY, Vol. 35, No. 1, p. 49–59 (January 1998)

Separation of Actinides from Rare Earth Elements by Electrorefining in LiCl–KCl Eutectic Salt

Yoshiharu SAKAMURA*,†, Takatoshi HIJIKATA*, Kensuke KINOSHITA*, Tadashi INOUE*,
T. S. STORVICK**, C. L. KRUEGER**, L. F. GRANTHAM***,
S. P. FUSSELMAN***, D. L. GRIMMETT*** and J. J. ROY***

* *Central Research Institute of Electric Power Industry (CRIEPI)*
** *Missouri University Research Reactor, University of Missouri-Columbia*
*** *Rocketdyne Division, Boeing North American*

(Received March 11, 1997), (Revised September 2, 1997)

A pyrometallurgical partitioning technology to recover actinides from high level radioactive wastes is being developed. In the process, actinides are separated from fission products by electrorefining in molten chloride systems. It is expected that REs (rare earth elements), main components of fission products are hardly separated from actinides. In order to estimate separation factors, electrorefining experiments to recover actinides from LiCl–KCl eutectic salt containing actinide (U, Np, Pu and Am) and RE (Y, La, Ce, Nd and Gd) chlorides were carried out at 450°C. Actinides were removed from a liquid cadmium anode and recovered as metal on a solid cathode. Typical cathode deposits were rough in appearance and contained 70–90 wt% adhering salt. The current efficiency was low because some of the deposit occasionally fell from the cathode. It is shown that uranium, neptunium and plutonium are relatively easily separated from REs and that americium is accompanied by some of REs.

KEYWORDS: high level radioactive wastes, pyrometallurgical partitioning, actinides, rare earth elements, molten salts, LiCl–KCl eutectics, electrorefining, solid cathode, liquid cadmium anode, separation process

I. Introduction

The pyrometallurgical partitioning technology to recover actinides from HLW (high level radioactive wastes) generated in PUREX reprocessing facility is being developed at CRIEPI (Central Research Institute of Electric Power Industry)(1)-(3). The process consists of four main steps: (1) denitration of HLW to oxides by heating, (2) chlorination to convert oxides to chlorides, (3) reductive extraction to reduce actinides in a molten salt by lithium metal and to extract them into liquid cadmium, (4) electrorefining in LiCl–KCl eutectic salt to separate actinides from liquid cadmium anode. The steps of (3) and (4) are illustrated in **Fig. 1**.

Elements contained in HLW are classified into three groups based on Gibbs free energies of formation of the chlorides (ΔG_f): (I) active metals such as alkali metal, alkaline earth, samarium and europium ($\Delta G_{f(450^\circ\mathrm{C})}<-300\,\mathrm{kJ/eq\text{-}Cl}$); (II) actinides and most of REs (rare earth elements) ($-300<\Delta G_{f(450^\circ\mathrm{C})}<-200\,\mathrm{kJ/eq\text{-}Cl}$); (III) noble metals such as ruthenium, technetium and molybdenum ($\Delta G_{f(450^\circ\mathrm{C})}>-200\,\mathrm{kJ/eq\text{-}Cl}$). Active metals remain in the salt during the reductive extraction step and noble metals remain in the cadmium anode during the electrorefining step as shown in Fig. 1. They are separated from actinides quite easily. Since REs are chemically similar to actinides and the amount of REs in HLW is much more than that of actinides, it is comparatively difficult to separate REs from actinides. Therefore it is very im-

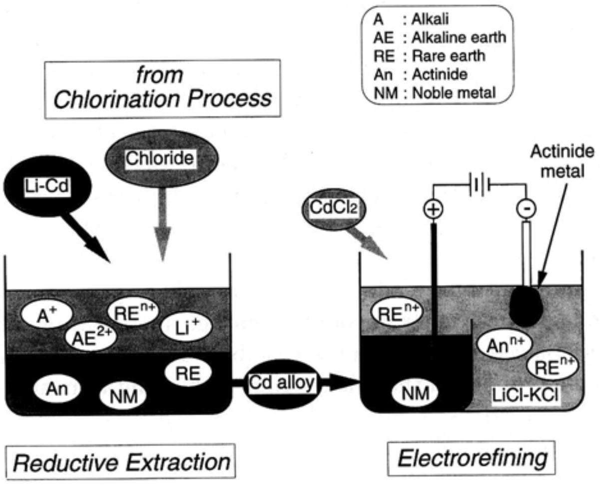

Fig. 1 Schematic actinide separation process in a molten salt/liquid cadmium system

---

* *Iwato-kita, Komae-shi 201.*

** *Columbia, Missouri 65211, U.S.A.*

*** *6633 Canoga Av., Canoga Park, California 91303, U.S.A.*

† Corresponding author, Tel. +81-29-264-8422,
Fax. +81-29-264-8478,
E-mail: sakamura@popsvr.tokai.jaeri.go.jp
Present address: Oarai Res. Establishment, Japan Atomic Energy Research Institute, *Oarai-machi, Higashiibaraki-gun, Ibaraki-ken 311-13.*

portant for the pyrometallurgical partitioning technology to estimate separation efficiency between actinides and REs during the electrorefining step. Standard potentials of REs in LiCl–KCl eutectic are slightly more negative than those of actinides(4)(5), and it follows that actinides can be deposited at a cathode while REs remain in salt.

This paper describes the electrorefining experiments to separate actinides from molten chloride/liquid cadmium systems containing actinides and REs. First, a series of preliminary solid cathode tests were carried out by using LiCl–KCl eutectic salt containing one of actinides (U, Np, Pu or Am) and two of REs (Nd and Gd). These two REs were chosen since neodymium is the RE of the highest yield and the standard potential of gadolinium is closest to those of the actinides. Subsequently, cadmium anode/solid cathode tests were carried out by using LiCl–KCl eutectic salt containing mixed actinides (U, Np, Pu and Am) and REs (Y, La, Ce, Nd and Gd).

II. Experimental

1. Reagents

High purity LiCl–KCl eutectic (58:42 mol%), $CdCl_2$ of 99.99% purity and rare earth chlorides of 99.99% purity were obtained from Anderson Physics Laboratory. Cadmium metal with a purity of 99.999% was obtained from Johnson-Matthey. Prior to experiments, cadmium was melted and the oxide at the surface was removed by pouring only the liquid metal into a stainless steel tray. Actinide metals were supplied by the U.S. Department of Energy and were >99.9% pure. Actinide-cadmium alloys were prepared by dissolving actinide metals in cadmium and removing the oxides at the surface of alloys. Actinide chlorides were prepared by oxidizing actinide-cadmium alloy in LiCl–KCl eutectic salt by adding $CdCl_2$ at 450 to 500°C [$2An(Cd)+3CdCl_2 \rightarrow 2AnCl_3(LiCl\text{–}KCl)+3Cd$, where An denotes an actinide].

2. Solid Cathode Tests with a Single Actinide and Two REs (An/Nd/Gd tests)

(1) Apparatus

The electrorefining apparatus is shown schematically in **Fig. 2**. The LiCl–KCl eutectic solution of one actinide and two RE chlorides was contained in a tantalum tube (13 mm dia.). A cathode of 1mm tantalum wire, a stirrer and a Ag/AgCl reference electrode (mole fraction of AgCl in LiCl–KCl eutectic was 0.00487) were immersed in the solution. The tantalum tube was immersed in a LiCl–KCl eutectic bath, which was contained in an alumina crucible. A counter electrode of lithium-antimony alloy, a secondary Ag/AgCl electrode and a type-K thermocouple sheathed in tantalum were also placed in the alumina crucible. The tantalum tube had a pinhole on the side covered with a tantalum shroud that served as a salt bridge. The cell was located in a stainless-steel thermowell attached to the floor of a glove box. The glove box atmosphere was high-purity argon containing <1 ppm O_2 and <1 ppm H_2O. The thermowell was heated externally with an electric furnace and temperature in the crucible was maintained at 450±1°C. Electrodepositions were performed by use of an EG&G PAR Model 273 potentiostat/galvanostat controlled by a Hewlett-Packard HP 9825T data acquisition system. Samples of salt, cadmium and cathode deposit were dissolved in water or nitric acid and the content of each element in the solutions was determined by a Baird PSX/262477-867A inductively coupled plasma atomic emission spectrometer (ICP-AES).

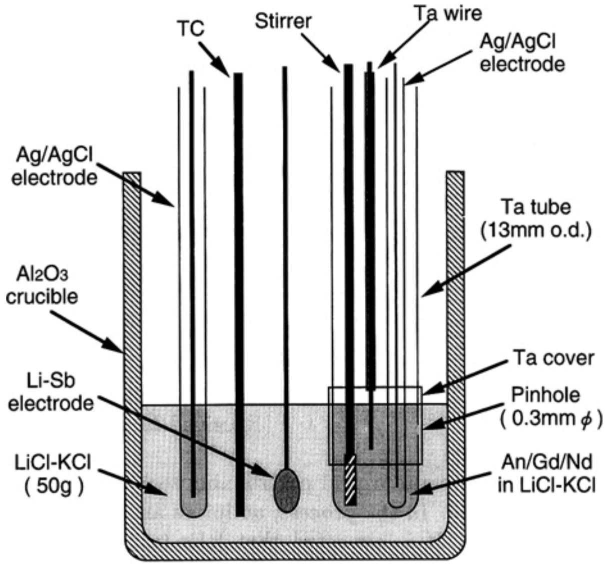

Fig. 2 Electrorefining cell for An/Nd/Gd tests

(2) Procedure

The assembled apparatus except for the 13 mmϕ tantalum tube was placed in the thermowell. The temperature was controlled at 450°C. Then the tantalum tube containing about 6 g of LiCl–KCl eutectic, 20 to 30 mg of actinide chloride, $NdCl_3$ and $GdCl_3$ was immersed into the alumina crucible containing about 50 g of LiCl–KCl eutectic. The level of the salt in the tantalum tube was adjusted to that of the outer crucible salt in order to avoid flow across the ionic conduction hole. The salt in the tantalum tube was stirred and the initial salt sample was taken.

Electrodepositions were carried out during the course of each electrorefining test. The deposition took place at 1 to 5 mA/cm^2 for 3 to 5C. The cathode potential (*vs.* the internal Ag/AgCl reference electrode) was monitored during the depositions. After each deposition the cathode was taken out from the melt and cut off at just above the deposit for analysis. A sample of the salt was also taken by dipping a tantalum wire shortly into the solution to collect adhering salt. A new cathode was installed and the electrodeposition procedure was repeated until the actinide content of the salt decreased below the analytical detection limit.

The cathode deposits were generally rough in appearance and contained at least 70% adhering salt by weight. The corrected metal content of the cathode deposit (W'_M) was calculated from

$$W'_M = W_M - W_S \cdot C_M, \qquad (1)$$

where W_M is the amount of metal in the deposit, W_S the amount of adhering salt and C_M the concentration of metal in the bulk salt. W_S was determined from the potassium content of the deposit.

3. Cadmium Anode/Solid Cathode Test with Mixed Actinides (U, Np, Pu and Am) and REs (Y, La, Ce, Nd and Gd) (Mixed Actinides/REs Test)

(1) Apparatus

The electrorefining apparatus is shown schematically in **Fig. 3**. The LiCl–KCl eutectic solution of actinide and RE chlorides was contained in a tantalum tube (13 mm dia.) which was immersed in a LiCl–KCl eutectic bath contained in an alumina crucible (not shown in Fig. 3). During the anode stripping test, a cathode of 1 mm tantalum wire in a closed-end alumina catch tube (6 mm dia.), a large cadmium pool used as the anode and a stirrer were placed inside (Fig. 3(a)). The alumina catch tube had a small window cut on one side and a small cadmium pool to catch any deposits that fell from the cathode.

During the salt stripping test, the large cadmium pool was removed and Li–Sb alloy was employed as the anode (Fig. 3(b)). The Li–Sb anode was surrounded by an alumina tube which had an ionic conduction slit in the side. A cathode of 1 mm tantalum wire and the same stirrer used in the anode stripping were also placed in the tantalum tube. During the electrolysis lithium in the Li–Sb anode was oxidized. According to the potential of Li–Sb alloy, Li–Sb alloy does not react with actinide and RE chlorides except UCl_3 spontaneously(5)(6). Under the salt stripping test condition, UCl_3 concentration was so low that UCl_3 might be hardly reduced by Li–Sb alloy.

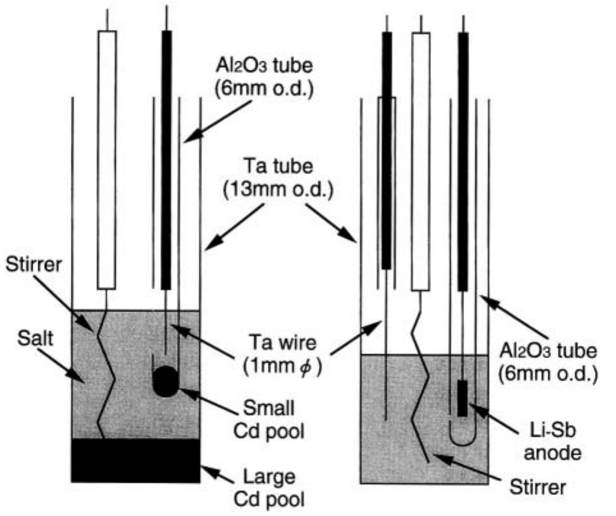

(a) Cell for anode stripping (b) Cell for salt stripping

Fig. 3 Electrorefining cell for mixed actinides/REs tests

(2) Procedure

Actinide-cadmium alloys, cadmium metal, RE chlorides and LiCl–KCl eutectic were put in a tantalum tube and it was placed in a LiCl–KCl eutectic bath with the temperature controlled at 450°C. The amounts of actinides and REs were selected to give the same ratio as the PUREX waste with two exceptions: uranium was present at about 1/4 amount and praseodymium was not added since it interfered with plutonium in ICP-AES analysis. After the salt and cadmium melted, electrodes and a stirrer were immersed. The salt and cadmium phases were allowed to equilibrate: some actinides were oxidized into the salt and some REs were reduced into the liquid cadmium. Then electrodepositions were carried out, so that actinides and REs were electrochemically transferred from the cadmium pool anode to the solid cathode. Typical depositions took place at cathode current densities from 5 to 10 mA/cm^2 for 10 to 40C, and the voltage between the cadmium anode and the cathode was about 0.3 V. During the twelfth electrodeposition the voltage increased, suggesting that actinides in the large cadmium pool were almost depleted. A small amount of $CdCl_2$ was added in order to oxidize all of the remaining actinides out of the cadmium pool. The large cadmium pool was removed from the tantalum tube. The additional depositions were carried out by using a Li–Sb alloy anode to strip actinides from the salt as shown in Fig. 3(b).

III. Results and Discussion

1. An/Nd/Gd Tests

Initial compositions of the salts in four An/Nd/Gd tests are shown in **Table 1**. About 6 g of LiCl–KCl eutectic salt containing 10–20 mg of actinide, neodymium and gadolinium was prepared. The electrodepositions were carried out by constant current electrolysis while monitoring the cathode potential. If the cathode potential is too negative, a large amount of REs is reduced at the cathode and the separation factor between actinides and REs becomes small. Typical deposits were rough in appearance and contained 70–90 wt% adhering salt. **Tables 2**(a)–(d) show conditions of electrodepositions and weights of metals recovered at the cathodes corrected for salt contamination. The errors of the weights were estimated from the precision of ICP-AES analysis considered to be ±5%. The current efficiencies were calculated from the weights of metals (An, Nd and Gd).

The current efficiency for each electrodeposition in the U/Nd/Gd test was 30–60% when the uranium concentration in the salt was high. At the end of the series of electrodepositions, the current was decreased to 0.5 mA to prevent RE deposition. The current efficiencies at this condition were less than 10%. The low current efficiencies were mainly due to the cathode deposits falling into the salt. Also, reduction of trivalent neodymium to divalent neodymium ($Nd(III)+e^- \rightarrow Nd(II)$)(7) might affect the current efficiencies when electrodepositions were car-

Table 1 Compositions of initial and final salts in the tantalum tube and sum of metal recovered at cathodes in the An/Nd/Gd tests

Test		Initial salt composition, weight (mg)	Final salt composition, weight (mg)	Sum of metal recovered at cathode (mg)
U/Nd/Gd	LiCl–KCl	4,825		
	U	10.9	<0.2[†]	4.6
	Gd	9.7	8.2	0.7
	Nd	9.2	7.9	0.4
Np/Nd/Gd	LiCl–KCl	6,279		
	Np	13.0	<0.2[†]	13.9
	Gd	14.2	8.2	0.2
	Nd	12.3	6.6	0.2
Pu/Nd/Gd	LiCl–KCl	6,337		
	Pu	11.9	0.2	10.7
	Gd	14.9	9.9	0.6
	Nd	12.2	7.3	0.4
Am/Nd/Gd	LiCl–KCl	6,329		
	Am	18.9	0.2	13.1
	Gd	15.2	1.1	7.1
	Nd	12.8	3.0	2.3

[†] <ICP detection limit

Table 2 Conditions of electrodepositions and weights of metals recovered at cathodes corrected for salt contamination in the U/Nd/Gd, Np/Nd/Gd, Pu/Nd/Gd and Am/Nd/Gd tests

Current efficiencies were calculated based on the weights of metals.

(a) U/Nd/Gd test

Run No.	Condition of electrodeposition			Weight of metal recovered at cathode (μg)			Current efficiency (%)
	Potential (V *vs.* AgCl)	Coulomb	Current (mA)	U	Nd	Gd	
1	−1.53	1.6	1.00	453±24	4.0±1.3	4.1±1.4	36.2
2	−1.54	7.3	1.00	1,593±81	12±2	12±2	27.2
3	—	4.4	—	861±44	286±16	545±30	60.3
4	−1.61	5.0	0.88	1,503±76	28±5	28±5	38.4
5	−1.73	3.9	0.59	179±9	26±2	19±2	7.8
6	−1.97	2.3	0.50	4.6±0.2	18±2	22±2	3.7
7	−2.01	3.1	0.50	2.1±0.1	18±1	49±3	4.1
Total		27.6		4,595±234	392±30	680±44	27.7

(b) Np/Nd/Gd test

Run No.	Condition of electrodeposition			Weight of metal recovered at cathode (μg)			Current efficiency (%)
	Potential (V *vs.* AgCl)	Coulomb	Current (mA)	Np	Nd	Gd	
1	−1.68	4.1	2.00	1,904±98	39±4	35±4	60.5
2	−1.70	4.2	4.00	3,056±155	31±4	36±4	92.3
3	−1.71	4.3	3.00	3,260±164	27±4	29±4	94.8
4	−1.73	4.5	1.50	2,902±145	25±3	30±3	80.6
5	−1.81	3.9	0.40	1,620±81	38±4	44±5	54.5
6	−1.84	1.4	0.18	133±7	11±1	11±1	14.7
7	−1.83	5.4	0.28	864±43	26±3	29±3	21.3
8	−1.88	3.2	0.37	121±6	21±1	21±1	7.3
Total		31.0		13,860±699	218±24	235±27	57.4

—: Not recorded

(c) Pu/Nd/Gd test

Run No.	Condition of electrodeposition			Weight of metal recovered at cathode (μg)			Current efficiency (%)
	Potential (V *vs.* AgCl)	Coulomb	Current (mA)	Pu	Nd	Gd	
1	−1.76	4.9	2.00	3,460±186	127±17	147±20	95.3
2	−1.76	0.5	0.50	159±8	14±1	14±1	49.8
3	−1.77	0.5	2.00	200±11	10±2	14±2	52.7
4	−1.78	0.5	4.00	204±11	11±2	15±3	58.8
5	−1.79	0.5	8.00	411±22	18±3	24±4	112.2
6	−2.01	0.6	20.00	73±5	21±2	42±4	37.4
7	−1.96	0.9	20.00	80±5	12±2	19±3	16.7
8	−1.91	0.7	12.00	110±6	11±1	13±2	27.2
9	−1.79	5.0	4.00	2,287±117	29±6	69±10	59.1
10	−1.81	5.0	4.00	2,620±132	44±8	91±11	68.3
11	−1.85	5.0	2.00	753±38	35±3	51±4	21.5
12	−1.85	5.0	1.00	280±14	23±2	31±3	8.9
13	−1.84	4.5	0.85	100±5	30±2	30±2	5.2
14	−1.88	3.5	0.50	3.8±0.2	16±1	15±1	1.9
Total		37.1		10,738±560	402±53	574±69	40.0

(d) Am/Nd/Gd test

Run No.	Condition of electrodeposition			Weight of metal recovered at cathode (μg)			Current efficiency (%)
	Potential (V *vs.* AgCl)	Coulomb	Current (mA)	Am	Nd	Gd	
1	−1.91	5.0	4.0	43±3	31±2	29±3	3.3
2	−1.91	5.0	4.0	58±5	43±4	45±4	4.7
3	−1.95	3.0	10.0	1,111±58	32±4	148±10	55.8
4	−1.99	3.9	14.0	1,078±56	56±5	298±17	50.0
5	−1.86	1.1	1.8	17±2	13±1	13±1	6.5
6	−1.94	1.0	1.2	263±14	19±2	50±3	46.5
7	−1.94	1.0	4.3	165±9	14±1	29±2	28.1
8	−1.98	1.1	9.5	535±28	29±2	171±10	94.8
9	−2.03	1.2	21.0	257±14	63±5	179±11	64.5
10	−1.97	5.0	8.4	1,360±69	48±4	305±17	45.9
11	−1.89	4.1	1.0	20±2	16±1	20±2	2.3
12	−1.93	4.0	2.0	245±13	34±2	62±4	11.9
13	−1.94	5.1	3.0	1,707±86	35±3	183±10	47.9
14	−1.96	5.1	3.0	2,020±102	55±4	397±21	64.4
15	−1.97	5.0	3.0	1,286±65	62±5	435±24	49.1
16	−1.98	5.1	3.0	1,049±53	79±6	600±32	49.7
17	−1.97	5.1	2.5	534±27	78±6	434±24	31.5
18	−1.97	5.0	2.5	451±23	73±4	470±24	31.1
19	−1.97	5.0	2.0	102±5	51±3	224±12	12.7
20	−1.98	5.0	1.5	13±1	28±2	65±4	3.9
21	−1.98	6.0	1.5	221±11	62±4	383±20	18.2
22	−1.95	10.3	1.0	16±1	83±5	153±8	4.5
23	−2.05	15.9	5.0	516±26	1,321±69	2,425±122	48.5
Total		107.9		13,067±672	2,324±144	7,119±385	31.0

ried out at low current density in the negative potential region (*i.e.* less than about −1.7 V *vs.* Ag/AgCl). Current efficiencies in the Np/Nd/Gd and Pu/Nd/Gd tests were generally higher than those in the U/Nd/Gd test. It appeared that neptunium and plutonium deposits adhered to the tantalum wire cathode better than uranium deposits.

Figure 4 shows the composition of cumulative cathode deposit during the series of electrodepositions. In the U/Nd/Gd test, the first two deposits were highly pure uranium. During the third electrodeposition, the cathode potential happened to be more negative than the RE reduction potentials, so that some of REs deposited at the cathode. If the cathode potential had

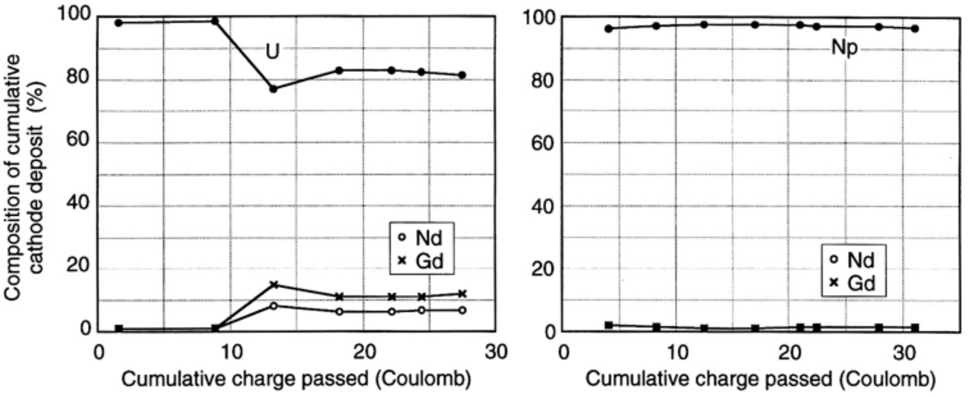

(a) U/Nd/Gd test **(b) Np/Nd/Gd test**

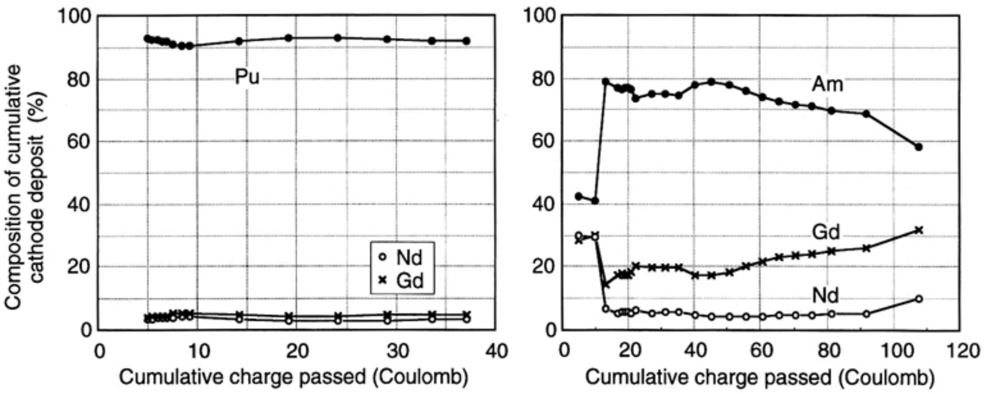

(c) Pu/Nd/Gd test **(d) Am/Nd/Gd test**

Fig. 4 Composition of cumulative cathode deposit during series of electrodepositions in An/Nd/Gd tests to separate actinides from $LiCl\text{-}KCl\text{-}AnCl_n\text{-}GdCl_3\text{-}NdCl_3$ systems at 450°C

been controlled appropriately, the separation would have been improved. In the Np/Nd/Gd and Pu/Nd/Gd tests more than 90 wt% of cumulative deposit was actinides. Consequently, it has been proved that uranium, neptunium and plutonium can be separated from REs at this condition.

In the americium test, the final REs content of the cumulative deposit was more than 40 wt%. Americium was more hardly separated from REs than uranium, neptunium and plutonium. The americium contents for the first two deposits were about 40% and the current efficiencies for these electrodepositions were extremely low as shown in Table 2(d). This seemed to be due to reduction of Am(III) to Am(II), since existence of Am(II) was reported by some workers(8)-(11). The amount of gadolinium in the deposits was larger than that of neodymium, since the standard potential of gadolinium is more positive than that of neodymium(5).

Figure 5 shows the concentration of metal chlorides in the salt. Actinide concentrations decreased satisfactorily as the electrodepositions proceeded. In the Np/Nd/Gd and Pu/Nd/Gd tests RE concentrations in the salt decreased, whereas there was a small amount of REs in the deposits as shown in Fig. 4. It is conjectured that some of REs reacted with impurities such as oxygen, moisture and tantalum oxide at the surface of the tantalum tube to form oxides or oxychlorides which were insoluble in the salt, and that some of REs diffused to the outer crucible through the pinhole for ionic conduction.

The final salt composition and the amount of metal recovered at the cathode are shown in Table 1. Finally almost all of actinides were depleted from the salt and more than 90% of neptunium and plutonium, 70% of americium and 40% of uranium were recovered.

2. Mixed Actinides/REs Test

Initial compositions of molten salt and liquid cadmium used in the mixed actinides/REs test are shown in **Table 3**. About 4.5 g of LiCl-KCl eutectic salt and about 6.3 g of cadmium metal were used as solvent. The initial compositions were determined by ICP-AES after actinides and REs were allowed to come to equilibrium between both phases. The distribution of each metal was consistent with the distribution coefficients obtained before(12)(13). The electrodepositions were carried out by constant current electrolysis while monitoring the voltage between the cathode and the anode. Typical deposits contained 70–90 wt% adhering salt. **Table 4**(a) shows conditions of electrodepositions and current efficiencies calculated from the amounts of metals recovered at the cathode, and Table 4(b) shows weights of metals recovered at the cathodes corrected for salt contamina-

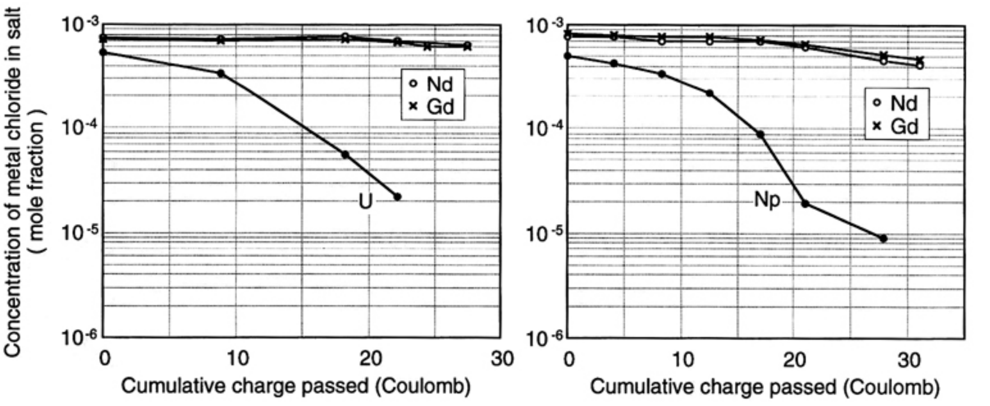

(a) U/Nd/Gd test

(b) Np/Nd/Gd test

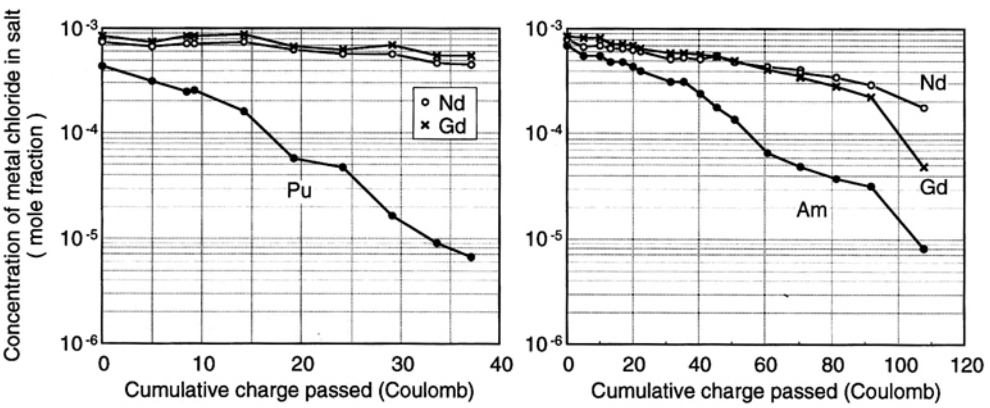

(c) Pu/Nd/Gd test

(d) Am/Nd/Gd test

Fig. 5 Concentration of metal chlorides in salt during series of electrodepositions in An/Nd/Gd tests to separate actinides from LiCl–KCl–$AnCl_n$–$GdCl_3$–$NdCl_3$ systems at 450°C

Table 3 Compositions of initial and final solutions and weight of each metal recovered in various samples in the mixed actinides/REs test

	Initial composition, weight (mg)		Final composition, weight (mg)		Sum of metal recovered at cathodes (mg)	Metal in small Cd pools (mg)	Metal in residue[†] (mg)	Metal in samples[††] (mg)	Mass balance, % metal accounted for $\frac{(C+D+E+F+G+H)}{(A+B)}\times 100$
	Salt phase A	Cd phase B	Salt phase C	Cd phase D	E	F	G	H	
LiCl–KCl	4,497								
Cd		6,331					202.5		
U	7.0	30.0	0.1	7.4	10.4	9.0	2.4	2.6	86
Np	6.0	9.0	0.1	0.5	9.9	2.4	1.3	1.6	105
Pu	0.8	0.8	0.0	0.2	0.3	0.3	0.6	0.4	107
Am	7.7	9.2	0.1	1.9	0.4	0.7	8.1	5.3	97
Y	11.7	0.0	3.8	0.0	0.6	0.1	1.0	5.3	92
La	35.9	0.5	6.7	0.1	0.6	0.5	9.1	14.1	85
Ce	66.1	2.9	3.4	0.5	2.7	2.6	30.4	25.5	94
Nd	101.8	5.2	3.6	0.8	3.8	3.9	48.6	41.0	95
Gd	7.0	0.3	0.4	0.0	1.1	0.2	2.2	3.0	94

[†] Residue recovered at the bottom of the tantalum tube might be a mixture of metal deposits, cadmium intermetallic compounds, oxides and oxychlorides.

[††] Salt samples, cadmium samples, Li–Sb anodes, and salts adhered to cathode deposits and small cadmium pools

tion. The errors of the weights were estimated from the precision of ICP-AES analysis considered to be ±5%. The errors of the RE weights during the first electrodepositions were relatively large because the deposits were contaminated with significant amounts of RE chlorides compared with the amounts of RE metals in the deposits

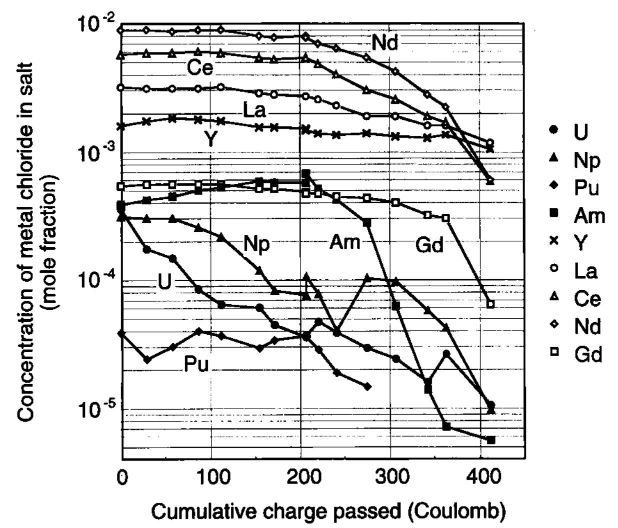

Fig. 6 Concentration of metal chlorides in salt in the mixed actinides/REs test

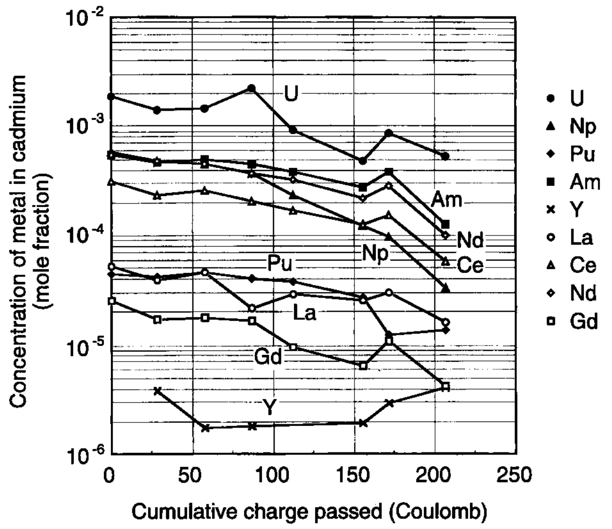

Fig. 7 Concentration of metals in liquid cadmium anode in the mixed actinides/REs test

(*cf.* Eq. (1)). The cathode current efficiencies were generally low because some of the deposits occasionally fell from the cathode. The presence of metal was found in the small cadmium pools under the cathodes and at the bottom of the tantalum tube as shown in Table 3. Since the small cadmium pools were used during the anode stripping test, the uranium and neptunium contents were high. The residue at the bottom of the tantalum tube might be a mixture of metal deposits, cadmium intermetallic compounds, oxides and oxychlorides. A small amount of cadmium was probably left when the large cadmium pool was removed. Because the system was not completely free from oxygen, oxides and oxychlorides would be formed. The average current efficiency computed from the decrease in the metal concentrations in the salt during the salt stripping test was about 85%. Table 3 shows that the mass balance for each metal was more than 85%.

Figure 6 shows the concentration of metal chlorides in the salt during the series of electrodepositions. The cadmium anode was replaced by a Li–Sb anode when 206C had been passed. The increase in actinide concentrations at 206C was due to a $CdCl_2$ addition designed to deplete the actinide and RE metals in the cadmium anode. Uranium and neptunium concentrations decreased during all of the electrodepositions. Americium concentration initially increased but after the anode replacement it decreased rapidly. When the cadmium anode was employed, more amount of americium was supplied from the anode than was reduced to metal at the cathode. The behavior of plutonium concentration was similar to that of americium. After 275C were passed, the plutonium concentration decreased below the analytical detection limit. The concentrations of REs were nearly constant during the first electrodepositions and then decreased after the anode replacement.

Figure 7 shows the concentration of metals in the cadmium anode. Actinide concentrations in the cadmium were relatively higher than those of REs. This is consistent with the results of the distribution coefficient experiments(12). Metals were removed gradually by the electrodepositions, and the current efficiency based on the metal content of the cadmium anode was about 20%. A significant amount of cathode deposit might drop back into the anode pool.

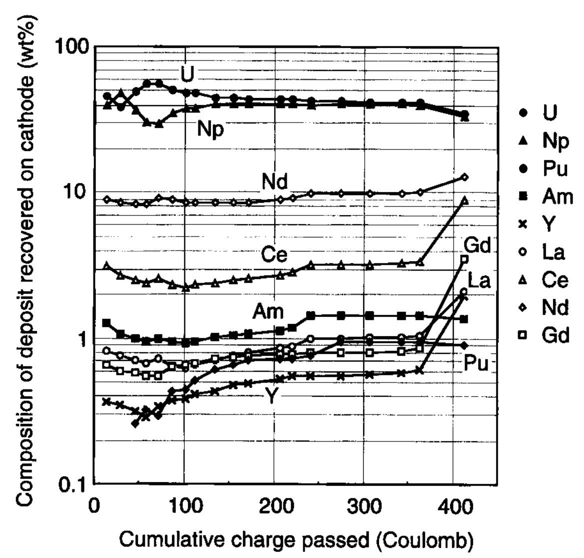

Fig. 8 Composition of cumulative deposit recovered at cathodes in the mixed actinides/REs test

Figure 8 shows the composition of cumulative deposit recovered at the cathodes. Uranium and neptunium were major components in the deposit. The americium content was 1–2 wt% and the RE content was 12–16 wt% throughout the experiment except the final electrodeposition in which a large amount of REs was deposited.

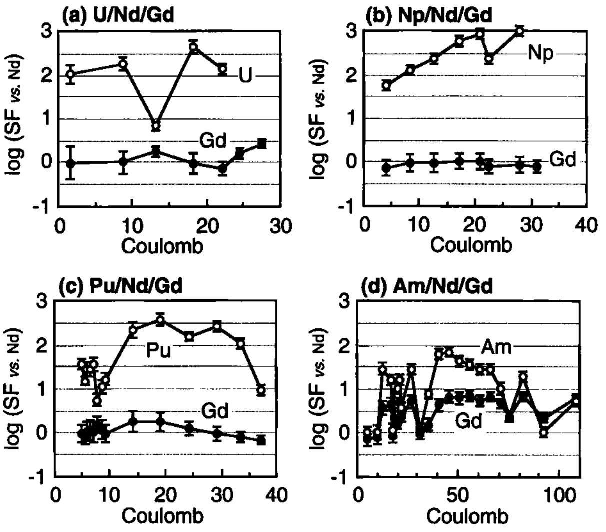

Fig. 9 Separation factor (*SF*) of actinides and gadolinium *vs.* neodymium for each electrodeposition in the An/Nd/Gd tests as a function of cumulative charge passed

Errors were estimated from the precision of ICP-AES analysis considered to be ±5%.

3. Separation Factor among Actinides and REs

In order to estimate the separation among actinides and REs, the separation factor (*SF*) is defined as

$$SF_{M1\ vs.\ M2}=\frac{(X_{M1\ \mathrm{in\ Deposit}})/(X_{M1\ \mathrm{in\ Salt}})}{(X_{M2\ \mathrm{in\ Deposit}})/(X_{M2\ \mathrm{in\ Salt}})} \quad (2)$$

where $X_{M\ \mathrm{in\ Deposit}}$ and $X_{M\ \mathrm{in\ Salt}}$ are mole fractions of *M* in a cathode deposit and in salt, respectively. Separation factor *vs.* neodymium in the An/Nd/Gd tests and in the mixed actinides/REs test are shown in **Fig. 9** and **Fig. 10**(a), respectively. The errors of *SF* for uranium, plutonium, americium and lanthanum were shown in Fig. 10(b). The errors for lanthanum were larger than those for any other elements in the mixed actinides/REs test. This is due to the correction for salt contamination as shown in Table 4(b). Generally, *SF* of actinides obtained in the mixed actinides/REs test are smaller than those obtained in the An/Nd/Gd tests. It is considered that the electrorefining conditions in the An/Nd/Gd tests using a single actinide were more suitable for the separation of each actinide from REs. In the mixed actinides/REs test, as the ratio of the amounts of REs to those of actinides was high, the difference between the reduction potentials of actinides and REs was small according to the Nernst equation. This made the separation difficult actually. The mass transfer limit of actinide ions may be also the reason, especially for plutonium of which concentration in the salt was extremely low during the test as shown in Fig. 6. Separation factor of actinides *vs.* neodymium in the mixed actinides/REs test was roughly estimated as follows: SF_{U}, $SF_{\mathrm{Np}}>100$; $SF_{\mathrm{Pu}}=10\text{–}30$; $SF_{\mathrm{Am}}=2\text{–}3$.

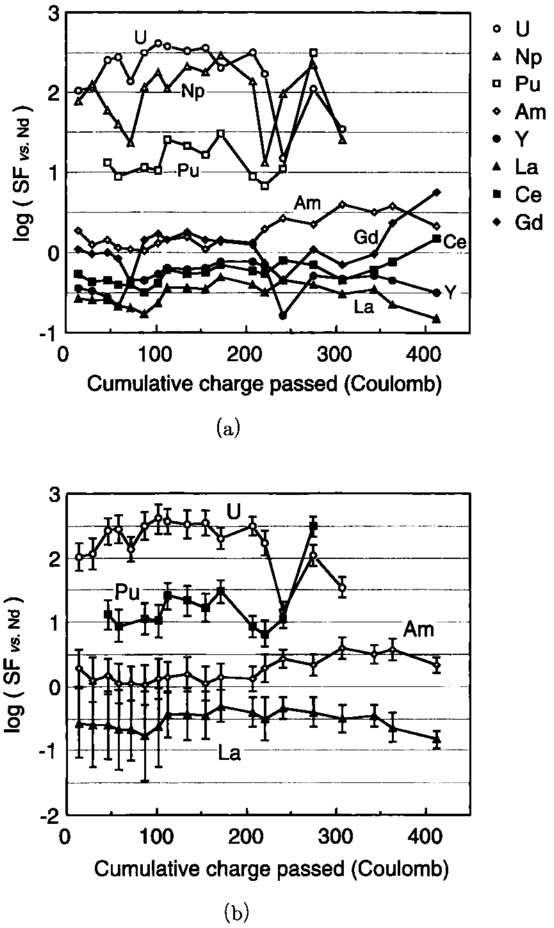

(a)

(b)

Fig. 10 (a) Separation factor (*SF*) of actinides and REs *vs.* neodymium for each electrodeposition in the mixed actinides/REs test as a function of cumulative charge passed. (b) Errors of the separation factors for uraniumn, plutonium, americium and lanthanum estimated from the precision of ICP-AES analysis considered to be ±5%

From the standard potentials of actinides and REs⁽⁴⁾⁽⁵⁾, the *SF* values should be much larger than obtained in the electrorefining experiments. Assuming that the activity of a metal in a deposit is equal to the mole fraction of the metal and that the deposit and the salt phase are at equilibrium, the relationship between *SF* and the difference in the standard potentials (ΔE) for two trivalent species is given by

$$\Delta E=\frac{RT}{3F}\ln SF, \quad (3)$$

where *R* is the gas constant, *T* the absolute temperature and *F* the Faraday constant. For example, ΔE for uranium and neodymium is about 0.58 V at 450°C, and $SF_{\mathrm{U}\ vs.\ \mathrm{Nd}}$ of 10^{12} is calculated by Eq. (3). The small values of *SF* in the experiments are possibly due to electrochemical polarization during the electrodepositions and underpotential deposition of REs of which the activity coefficients in the deposit are less than unity.

From Fig. 10, REs are arranged in decreasing order of *SF*: Gd>Nd>Ce, Y>La. This is consistent with the order of the standard potentials of REs.

Table 4 (a) Conditions of electrodepositions and current efficiencies calculated based on the weight of metals in the mixed actinides/REs test

Run No.	Condition of electrodeposition				Current efficiency (%)
	Anode	Cell voltage (V)	Current (mA)	Coulomb	
1	Cd	0.27	4.0	14.3	13.5
2	Cd	0.28	4.0	14.4	10.9
3	Cd	0.25	4.0	16.3	20.0
4	Cd	0.25	4.0	12.4	33.1
5	Cd	0.27	3.0	14.4	6.0
6	Cd	0.30	4.0	15.2	35.0
7	Cd	0.32	4.0	15.4	21.2
8	Cd	0.29	4.0	9.4	14.7
9	Cd	0.31	4.0	21.9	20.3
10	Cd	0.31	4.0	21.6	15.4
11	Cd	0.33	2.0	16.2	5.8
12	Cd	0.30	2.0	35.0	4.2
13	Li–Sb	0.22	2.0	13.7	3.9
14	Li–Sb	0.39	2.5	20.6	14.3
15	Li–Sb	0.39	2.5	33.9	1.6
16	Li–Sb	0.41	3.0	33.2	0.6
17	Li–Sb	0.47	3.0	35.0	0.4
18	Li–Sb	0.52	3.0	21.3	0.9
19	Li–Sb	0.58	3.0	48.0	21.3
Total				412.2	11.3

Table 4 (b) Weight of metals recovered at cathodes corrected for salt contamination in the mixed actinides/REs test

Run No.	Weight of metal recovered at cathode (μg)								
	U	Np	Pu	Am	Y	La	Ce	Nd	Gd
1	572±30	490±26	N.D.	16±2	4.6±2.7	10±8	39±16	111±27	8.2±1.9
2	356±19	668±35	N.D.	9.7±2.3	3.8±2.9	8.2±7.9	27±16	96±27	6.3±1.8
3	1,412±72	605±32	12±1	22±4	6.4±4.4	16±12	54±24	184±42	13±3
4	1,980±100	547±30	13±1	24±5	6.9±6.5	18±17	65±34	251±60	15±4
5	309±16	125±7	N.D.	11±2	6.0±2.0	7.3±4.9	27±10	105±19	3.1±1.1
6	1,638±83	1,834±95	29±2	33±7	18±8	19±22	72±45	336±78	33±6
7	902±46	1,288±66	12±1	21±4	11±5	13±12	45±25	168±43	19±3
8	410±21	413±21	16±1	13±2	7.3±1.9	12±5	37±10	95±17	9.1±1.3
9	1,038±52	1,786±91	36±2	44±7	19±6	32±16	89±32	258±56	32±5
10	1,034±52	977±50	23±1	31±6	18±5	28±13	86±26	231±44	23±3
11	140±7	354±18	16±1	13±1	6.8±1.2	12±3	34±6	73±10	7.1±0.8
12	364±18	326±16	10±1	25±2	14±2	20±4	60±9	156±18	13±1
13	132±7	16±1	3.2±0.2	16±2	5.7±1.1	7.7±2.9	25±6	70±11	3.8±0.7
14	34±2	220±11	12±1	66±4	4.7±1.2	35±4	111±10	223±19	7.9±1.0
15	34±2	238±12	49±2	6.6±0.5	2.8±0.5	4.6±0.9	13±2	34±4	3.2±0.3
16	11±1	35±2	4.8±0.2	3.4±0.2	3.2±0.5	4.6±1.0	10±2	35±3	2.5±0.3
17	N.D.	N.D.	N.D.	0.81±0.05	4.5±0.5	5.8±0.8	12±1	31±3	3.6±0.3
18	N.D.	N.D.	1.5±0.1	0.77±0.05	6.5±1.0	6.1±1.5	22±2	39±4	13±1
19	N.D.	16±1	32±2	43±2	431±25	361±24	1,821±94	1,319±69	836±42
Total	10,365±526	9,936±512	269±15	400±55	581±77	621±161	2,647±370	3,816±553	1,051±78

N.D.: Not Detected

IV. Conclusions

Electrorefining experiments were carried out in LiCl–KCl eutectic salt containing actinide and RE chlorides. The actinide metals were removed from a liquid cadmium anode and were recovered on solid cathodes. Typical cathode deposits were rough in appearance and contained 70–90 wt% adhering salt. The cathode current efficiencies were low because some of the deposit occasionally fell from the cathode. Finally almost all of the actinides were depleted from the salt by electrolysis using a lithium alloy anode. Further work will be needed for collecting deposits that fall from the cathode to improve current efficiency and recovery yield.

It has been proved that uranium, neptunium and plutonium can be separated from REs relatively easily and that americium is accompanied by some of REs. Separation factor of actinides *vs.* neodymium obtained in the electrorefining test of the HLW composition was roughly estimated as follows: SF_{U}, $SF_{\mathrm{Np}}>100$; $SF_{\mathrm{Pu}}=10\text{–}30$; $SF_{\mathrm{Am}}=2\text{–}3$. Rare earth elements are arranged in decreasing order of SF: Gd>Nd>Ce, Y>La. The results are consistent with the order of the standard potentials of actinides and REs.

In order to improve the separation of actinides from REs, the cathode potential should be less negative than the RE reduction potentials. When the actinide concentrations in the salt are low, the actinide reduction potentials are close to the RE reduction potentials and the electrochemical polarization is large. Thus, high current density will decrease SF of actinides from REs. However, the experimental results indicate that low current density causes low current efficiency, which is likely due to the reduction of Nd(III) to Nd(II).

ACKNOWLEDGMENTS

This study was performed with the assistance of Missouri University Research Reactor staffs. We wish to thank N. Takahashi and T. Higashi of Kawasaki Heavy Industries, Ltd. for their support of this program.

—REFERENCES—

(1) Inoue, T., Sakata, M., Miyashiro, H., Matsumura, M., Sasahara, A., Yoshiki, N.: *Nucl. Technol.*, **69**, 206 (1991).

(2) Sakata, M., Miyashiro, H., Inoue, T.: *Proc. Int. Conf. on Fast Reactors and Related Fuel Cycles*, Vol. II, 19–7 (1991).

(3) Inoue, T., Sakata, M, Kurata, M., Sakamura, Y., Hijikata, T., Kinoshita, K.: *IAEA-TECDOC*-783, p. 137 (1995).

(4) Krueger, C. L., Storvick, T. S., Roy, J. J., Grantham, L. F., McCoy, L. R., Inoue, T., Miyashiro, H., Takahashi, N.: *J. Electrochem. Soc.*, **138**, 1186 (1991).

(5) Sakamura, Y., Inoue, T., Storvick, T. S., Grantham, L. F.: *Proc. Int. Conf. on Evaluation of Emerging Nuclear Fuel Cycle Systems* (*Global'95*), Vol. 2, p. 1185 (1995).

(6) Weppner, W., Huggins, R. A.: *J. Electrochem. Soc.*, **125**, 7 (1978).

(7) Wu, I., Zhu, H., Sato, Y., Yamamura, T., Sugimoto, K.: *Proc. 9th Int. Symp. on Molten Salts, Electrochem. Soc.*, Vol. 94-13, p. 504 (1994).

(8) Ferris, L. M., Mailen, J. C., Smith, F. J.: *J. Inorg. Nucl. Chem.*, **33**, 1325 (1971).

(9) Mullins, L. J., Beaumont, A. J., Leary, J. A.: *J. Inorg. Nucl. Chem.*, **30**, 147 (1968).

(10) Leary, J. A., Mullins, L. J.: *J. Chem. Thermodyn.*, **6**, 103 (1974).

(11) Grimmett, D. L., Roy, J. J., Grantham, L. F., Krueger, C. L., Storvick, T. S., Sharp, P. R., Sorrell, D. A., Cooper, J. W., Inoue, T., Sakamura, Y., Takahashi, N.: *183rd Meeting Extended Abstracts, Electrochem. Soc.*, Vol. 93-1, p. 1984 (1993).

(12) Kurata, M., Sakamura, Y., Hijikata, T., Kinoshita, K.: *J. Nucl. Mater.*, **227**, 110 (1995).

(13) Sakata, M., Kurata, M., Hijikata, T., Inoue, T.: *J. Nucl. Mater.*, **185**, 56 (1991).
